Published by IOP Publishing for Sissa Medialab

Received: *November 28, 2017*
Revised: *January 4, 2018*
Accepted: *January 10, 2018*
Published: *January 24, 2018*

XII International Symposium on Radiation from Relativistic Electrons in Periodic Structures — RREPS-17
18–22 September, 2017
DESY, Hamburg, Germany

2018 JINST 13 C01032

Transition radiation on a superlattice in finite thickness plate generated by two acoustic waves

A.R. Mkrtchyan,[a,b] **V.V. Parazian**[c,1] **and A.A. Saharian**[c,d]

[a] *Tomsk Polytechnic University,*
30 Lenin Avenue, 634050 Tomsk, Russia
[b] *Belgorod National Research University,*
85 Pobedy Street, 308015 Belgorod, Russia
[c] *Institute of Applied Problems in Physics NAS RA,*
25 Nersessian Street, 0014 Yerevan, Armenia
[d] *Yerevan State University,*
1 Alex Manoogian Street, 0025 Yerevan, Armenia

E-mail: vparazian@gmail.com

Abstract: Forward transition radiation from relativistic electrons is investigated in an ultrasonic superlattice excited in a finite thickness plate by two acoustic waves. In the quasi-classical approximation formulae are derived for the vector potential of the electromagnetic field and for the spectral-angular distribution of the radiation intensity. Zone structures appear in the plate, which makes it possible (by an appropriate choice of the frequencies of the two acoustic waves) to control the spectral-angular distribution of the radiation through changes in the parameters of the medium. The acoustic waves generate new resonance peaks in the spectral and angular distribution of the radiation intensity. The heights of the peaks can be tuned by choosing the parameters of the acoustic waves. Numerical examples are presented for a plate of fused quartz.

Keywords: Cherenkov and transition radiation; Radiation calculations

[1] Corresponding author.

https://doi.org/10.1088/1748-0221/13/01/C01032

Contents

1 Introduction

The transition radiation is among the most interesting types of electromagnetic radiation emitted by a relativistic charged particle interacting with an inhomogeneous medium (for reviews see [1–4]). Because of its remarkable properties, the transition radiation has found a number of important applications. In particular, optical and extreme ultraviolet backward transition radiation was used for the measurement of transverse size, divergence, and energy of electron and proton beams (see [5, 6] and references therein). It is well known that the interference effects in periodic structures considerably increase the transition radiation intensity. In [7], it has been suggested to use ultrasonic waves for the generation of a periodic structure in the radiator of X-ray transition radiation. The optical transition radiation on a plate, in the presence of acoustic waves, is investigated in [8] and [9] for the cases of normal and oblique incidence of the radiating particle. The transition radiation on a dynamic periodic interface between two dielectric media has been recently discussed in [10].

In the present paper we consider the transition radiation on a plate excited by two acoustic waves. As it will be shown, the presence of the second wave provides additional tools for the control of spectral and angular characteristics of the radiation.

2 Vector potential for the radiation field

We consider a plate with thickness l immersed in a homogeneous medium with dielectric permittivity ε_1. The axis z will be directed along the normal to the boundaries of the plate, located at $z = -l$ and $z = 0$. We assume the presence of acoustic field inside the plate generated by two acoustic waves with the wavelengths λ_{s1} and λ_{s2} and propagating along the axis z. The acoustic waves give rise to the modulation of dielectric permittivity of the plate in the form

$$\varepsilon(z) = \varepsilon_0 + \sum_{j=1,2} \Delta\varepsilon_j \cos\left(k_{sj} z + \omega_{sj} t + \psi_j\right), \tag{2.1}$$

where $-l < z < 0$, ε_0 is the dielectric permittivity in the absence of the acoustic field, $k_{sj} = 2\pi/\lambda_{sj}$, $\omega_{sj} = 2\pi\nu_{sj}$, ν_{s1} and ν_{s2} are the frequencies of the acoustic waves.

In the present paper we are interested in the transition radiation from a charge e (electron) moving along the axis z with a constant velocity $\mathbf{v} = v\mathbf{n}_z$. The transition radiation is formed on the boundaries of the plate and on the one-dimensional superlattice described by (2.1). The exact solution of the problem is complicated and we will make simplifying assumptions. First of all, assuming that $\nu_{sj} l/v \ll 1$, the dynamical nature of the dielectric permittivity can be ignored and the problem can be approximated by the one for a static superlattice. For relativistic electrons and for the plate thickness $l \lesssim 1$ cm this condition is obeyed in relatively wide range for frequencies of the acoustic waves, $\nu_{sj} \ll 10^{11}$ Hz. Next, we assume that the amplitudes $\Delta\varepsilon_j$ are relatively small. Let us denote by ω the radiation frequency. Under the condition $\omega \gg k_{sj}c$, with ω being the radiation frequency, we can use the quasi-classical approximation for the evaluation of the radiation field in the forward direction.

In the Lorentz gauge, for the vector potential of the electromagnetic field one has $\mathbf{A} = A(\mathbf{r},t)\mathbf{n}_z$. This determines the radiation polarization: the magnetic field is perpendicular to the plane containing the photon wave vector and the vector $\mathbf{n}_z$. In the discussion below the calculations will be presented for the Fourier component

$$A(\mathbf{k}_\perp, \omega, z) = \frac{1}{(2\pi)^3} \int_{-\infty}^{+\infty} dx \int_{-\infty}^{+\infty} dy \int_{-\infty}^{+\infty} dt\, A(\mathbf{r},t)\, e^{i(\omega t - k_1 x - k_2 y)}, \tag{2.2}$$

with $\mathbf{k}_\perp = (k_1, k_2)$. In the quasi-classical approximation, the Fourier component in the region $z > 0$ is determined by the expression

$$A(\mathbf{k}_\perp, \omega, z) = \frac{iev}{4\pi^2 c} \sqrt{\frac{\varepsilon_1}{k_3^{(1)}}} \int_{-\infty}^{+\infty} dt\, [k_3(z(t))\varepsilon(z(t))]^{-1/2} \exp\left[i\omega t + i\int_{z(t)}^{z} k_3(z')dz'\right], \tag{2.3}$$

where $z(t) = -l + v(t - t_0)$ is the z-coordinate of the charge, $k_3^{(n)} = \sqrt{\omega^2\varepsilon_n/c^2 - k_\perp^2}$, $n = 0, 1$. The function $\varepsilon(z)$ is defined as $\varepsilon(z) = \varepsilon_1$ in the regions $z < -l$, $z > 0$, and as $\varepsilon(z) = \varepsilon_0 + \sum_{j=1,2} \Delta\varepsilon_j \cos\left(k_{sj}z + \varphi_j\right)$ inside the plate, $-l < z < 0$, where $\varphi_j = \omega_{sj}t_0 + \psi_j$. The function $k_3(z)$ is given by $k_3(z) = k_3^{(1)}$ for $z < -l$, $z > 0$, and

$$k_3(z) = k_3^{(0)} + \sum_{j=1,2} a_j k_{sj} \cos\left(k_{sj}z + \varphi_j\right), \tag{2.4}$$

for $-l < z < 0$, with the notation $a_j = \omega^2\Delta\varepsilon_j/(2c^2 k_{sj} k_3^{(0)})$.

The evaluation of the vector potential by the formula (2.3) is similar to that for the case of a single acoustic wave and we will omit the details. In the region $z > 0$ one gets

$$A(\mathbf{k}_\perp, \omega, z) = \frac{ie}{2\pi^2 c} \sqrt{\frac{\varepsilon_1}{k_3^{(1)}}} e^{i\omega(t_0 + l/v) + ik_3^{(1)}z} \left\{ \frac{e^{i(a_1 \sin\varphi_1 + a_2 \sin\varphi_2)}}{\sqrt{k_3^{(0)}\varepsilon_0}} \sum_{m_1, m_2 = -\infty}^{+\infty} J_{m_1}(a_1) J_{m_2}(a_2) \right.$$
$$\left. \times\, e^{-\frac{i}{2}l(\frac{\omega}{v} - k_{m_1,m_2}) - i(m_1\varphi_1 + m_2\varphi_2)} \frac{\sin[l(\omega/v - k_{m_1,m_2})/2]}{\omega/v - k_{m_1,m_2}} + \frac{e^{i\phi - il(\omega/v - k_3^{(1)})} - 1}{2i\sqrt{k_3^{(1)}\varepsilon_1}(\omega/v - k_3^{(1)})} \right\}. \tag{2.5}$$

Here we have introduced the notation $k_{m_1,m_2} = k_3^{(0)} + \sum_{j=1,2} m_j k_{sj}$ and ϕ is defined by the relation

$$\phi = (k_3^{(0)} - k_3^{(1)})l + 2\sum_{j=1,2} a_j \sin\left(k_{sj}l/2\right)\cos\left(\varphi_j - k_{sj}l/2\right). \tag{2.6}$$

In the special case $\Delta\varepsilon_1 = \Delta\varepsilon_2$, $k_{s1} = k_{s2}$, $\varphi_1 = \varphi_2$, one has $a_1 = a_2$ and instead of m_2 we introduce in (2.5) a new summation variable $m = m_1 + m_2$. For a given m, the summation over m_1 is done by using the formula $J_m(2a_1) = \sum_{m_1=-\infty}^{+\infty} J_{m\mp m_1}(a_1)J_{m_1}(a_1)$ and from (2.5) we obtain the corresponding result for a single acoustic wave with the amplitude of the oscillations $2\Delta\varepsilon_1$, discussed in [8].

3 Spectral-angular distribution of the radiation intensity

Let us introduce the angle θ between the momentum of the radiated photon and the axis z. Having the Fourier transform $A(\mathbf{k}_\perp, \omega, z)$ for the vector potential, we can evaluate the energy radiated in the forward direction during the electron transit time in the range of frequencies $d\omega$ and angles $d\theta$, denoted here by $I(\omega,\theta)\,d\omega d\theta$. For the corresponding energy density in the region $z \gg l$ one has [1]

$$I(\omega,\theta) = (2\pi)^3 \varepsilon_1^{3/2} c^{-3}\omega^4 \sin^3\theta\cos^2\theta\,|A(\mathbf{k}_\perp,\omega,z)|^2. \tag{3.1}$$

In accordance with the definition of the angle θ we have $|\mathbf{k}_\perp| = k_\perp = (\omega\sqrt{\varepsilon_1}/c)\sin\theta$. For the beam of relativistic electrons, the expression $I(\omega,\theta)$, with the vector potential taken from (2.5), should be averaged over the phases φ_1 and φ_2.

First we consider the case when the phases for separate waves are not correlated and the averaging procedure is done separately for φ_1 and φ_2. After averaging, the spectral-angular density of the radiated energy in the angular region $\sin\theta < \sqrt{\varepsilon_0/\varepsilon_1}$ is presented as

$$I(\omega,\theta) = \frac{2e^2\beta_1^2}{\pi c\sqrt{\varepsilon_1}}\sin^3\theta\left\{\sum_{m_1,m_2=-\infty}^{+\infty} J_{m_1}^2(a_1)J_{m_2}^2(a_2)\frac{\sin^2[g_{m_1,m_2}(\theta)l\omega/2v]}{g_{m_1,m_2}^2(\theta)}\right.$$
$$\left.\times\left[\sqrt{\frac{\varepsilon_1\cos\theta}{\varepsilon_0\sqrt{\varepsilon_0/\varepsilon_1 - \sin^2\theta}}} - \frac{g_{m_1,m_2}(\theta)}{1-\beta_1\cos\theta}\right]^2\right\}, \tag{3.2}$$

where and in what follows $\beta_j = v\sqrt{\varepsilon_j}/c$, $j = 0, 1$. In this expression we have introduced the notation

$$g_{m_1,m_2}(\theta) = 1 - \beta_1\sqrt{\varepsilon_0/\varepsilon_1 - \sin^2\theta} - \sum_{j=1,2} m_j k_{sj} v/\omega. \tag{3.3}$$

For the arguments of the Bessel functions one has the expression

$$a_j = \omega\Delta\varepsilon_j/[2ck_{sj}\sqrt{\varepsilon_0 - \varepsilon_1\sin^2\theta}], \tag{3.4}$$

for $j = 1, 2$. In this expression, $\omega/(ck_{sj}) = \lambda_{sj}/(\lambda\sqrt{\varepsilon_1})$, where $\lambda = 2\pi c/(\omega\sqrt{\varepsilon_1})$ is the radiation wavelength in the medium with the permittivity ε_1. Though $|\Delta\varepsilon_j|$ is small, the arguments a_j, in general, are not small. For $\Delta\varepsilon_2 = 0$, in (3.2) the term with $m_2 = 0$ survives only and the corresponding formula is reduced to the one for the problem with a single acoustic wave.

2018 JINST 13 C01032

For a fixed radiation wavelength, in (3.2) there are angular peaks $\theta = \theta_{m_1,m_2}(\lambda)$ corresponding to the zeros of the function $g_{m_1,m_2}(\theta)$. These peaks are present under the conditions

$$\frac{1}{\beta_1} - \sqrt{\frac{\varepsilon_0}{\varepsilon_1}} \leqslant \lambda \sum_{j=1,2} \frac{m_j}{\lambda_{sj}} \leqslant \frac{1}{\beta_1}, \tag{3.5}$$

and the corresponding angular locations are determined from

$$\sin^2 \theta_{m_1,m_2}(\lambda) = \varepsilon_0/\varepsilon_1 - (1/\beta_1 - m_1\lambda/\lambda_{s1} - m_2\lambda/\lambda_{s2})^2 . \tag{3.6}$$

For the radiation inside the plate the locations of the angular peaks are given by

$$\theta = \theta^{(0)}_{m_1,m_2}(\lambda_0) = \arccos\left(1/\beta_0 + m_1\lambda_0/\lambda_{s1} + m_2\lambda_0/\lambda_{s2}\right), \tag{3.7}$$

where $\lambda_0 = 2\pi c/(\omega\sqrt{\varepsilon_0})$ is the radiation wavelength in the medium with the permittivity ε_0. After the refraction on the boundary at $z = 0$, the corresponding outgoing angle for the radiation in the region $z > 0$ is determined by the relation $\sin\theta = \sqrt{\varepsilon_0/\varepsilon_1}\,\sin[\theta^{(0)}_{m_1,m_2}(\lambda_0)]$ which coincides with $\theta_{m_1,m_2}(\lambda)$. Note that the angular and frequency locations of the peaks are determined by the periodicity properties of the geometry under consideration and do not depend on the specific profile of the inhomogeneities. The profile determines the distribution of the radiation intensity among the peaks.

In the special case $\Delta\varepsilon_1 = \Delta\varepsilon_2 = 0$, the only nonzero contribution in (3.2) comes from the term with $m_1 = m_2 = 0$ and we obtain the transition radiation intensity in a finite thickness plate in the absence of acoustic waves, described in the quasi-classical approximation. The comparison with the exact formula in a more general case of oblique incidence has been made in [9] (for the validity of the quasi-classical approximation see also [1]). In the absence of acoustic waves, the location of the corresponding angular peak is obtained from (3.6) putting $m_1 = m_2 = 0$. As seen from (3.6), the presence of acoustic waves leads to additional peaks. The locations of the peaks can be controlled by tuning the wavelengths λ_{sj}.

In figure 1, for the electron energy 50 MeV and for uncorrelated phases of acoustic waves we have plotted the angular and wavelength dependence of the quantity $I(\omega,\theta)/\hbar$ (given by (3.2)) for a plate made of fused quartz with the thickness $l = 1$ cm. We have taken $\varepsilon_1 = 1$ and for the dielectric permittivity of the plate, $\varepsilon_0 = \varepsilon_0(\omega)$, the Sellmeier dispersion formula is used. The frequencies for separate acoustic waves are taken as $\nu_{s1} = 10$ MHz and $\nu_{s2} = 20$ MHz. For the amplitudes of the electron number density induced by the acoustic waves we have taken $\Delta n_1/n_0 = 0.05$ and $\Delta n_2/n_0 = 0.025$, where n_0 is the electron number density in the absence of acoustic waves. As it has been already mentioned before, the presence of acoustic waves gives rise to new peaks in both the angular and spectral distributions of the radiation intensity. The left panel in figure 1 presents the angular dependence for a fixed radiation frequency corresponding to $\nu = \omega/(2\pi) = 6.0624 \times 10^{13}$Hz (radiation wavelength $\lambda = 4.944 \times 10^{-4}$cm). This frequency is chosen to obtain the suppression of the radiation at the angular peak in the absence of acoustic waves, corresponding to $\sin^2\theta_{0,0} = \varepsilon_0(\omega)/\varepsilon_1 - 1/\beta_1^2$ (the argument of the function $J_0^2(a_1)$ is close to the first zero of the Bessel function $J_0(x)$). For the parameters under consideration $\theta_{0,0} \approx 1.115$ rad. The other angular peaks in figure 1 are generated by the presence of acoustic waves. There are also peaks outside the angular range depicted in figure 1. However, their heights are much less than those presented on the figure. The same is the case for the radiation near the small angles

2018 JINST 13 C01032

$\theta \sim \sqrt{1 - v^2/c^2}$. On the right panel of figure 1 we have plotted the dependence of $I(\omega, \theta)/\hbar$ on the radiation wavelength λ for fixed $\theta = 1.094$ rad. This value of the radiation angle corresponds to the peak on the left panel. The locations of the peaks and their heights can be controlled by tuning the parameters of the acoustic field. Note that, in the approximation we have used, the locations of the angular peaks do not depend on the amplitudes of the acoustic waves.

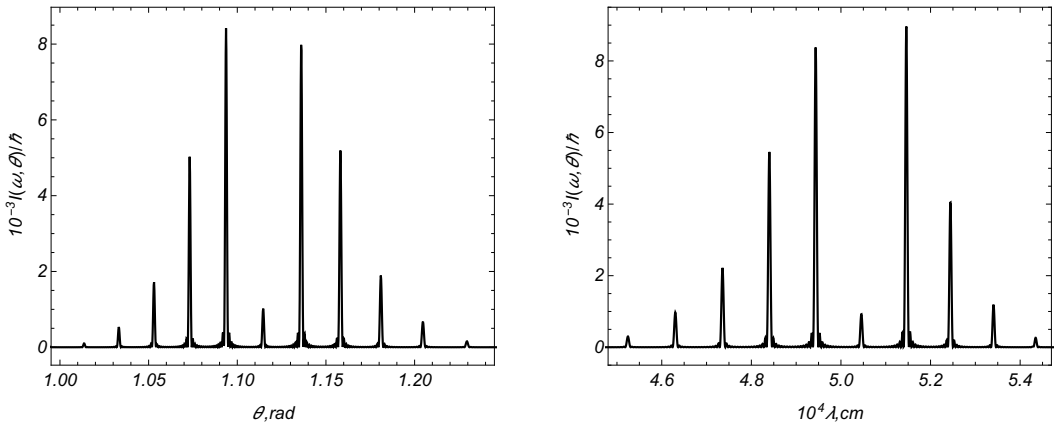

Figure 1. The angular (left panel) and wavelength (right panel) dependence for the intensity of the transition radiation on a plate made of fused quartz excited by two acoustic waves with uncorrelated phases.

Now let us consider the case when the phase shift between two acoustic waves is fixed, $\varphi_2 = \varphi_1 + \varphi$. Averaging over φ_1 for a given φ, the spectral-angular density of the radiated energy is presented in the form

$$I(\omega,\theta) = \frac{2e^2\beta_1^2}{\pi c\sqrt{\varepsilon_1}} \sin^3\theta \left\{ \frac{\varepsilon_1 \cos\theta}{\varepsilon_0\sqrt{\varepsilon_0/\varepsilon_1 - \sin^2\theta}} \sum_{m_j,m=-\infty}^{+\infty} J_{m_1}(a_1) J_{m_1+m}(a_1) J_{m_2}(a_2) J_{m_2-m}(a_2) \right.$$
$$\times \cos\left[m\left(l\Delta k_s/2 + \varphi\right)\right] \frac{\sin[g_{m_1,m_2}(\theta) l\omega/2v]}{g_{m_1,m_2}(\theta)} \frac{\sin[(g_{m_1,m_2}(\theta) - mv\Delta k_s/\omega) l\omega/2v]}{g_{m_1,m_2}(\theta) - mv\Delta k_s/\omega}$$
$$\left. \times \left(1 - 2\sqrt{\frac{\varepsilon_0\sqrt{\varepsilon_0/\varepsilon_1 - \sin^2\theta}}{\varepsilon_1\cos\theta}} \frac{g_{m_1,m_2}(\theta) - mv\Delta k_s/\omega}{1 - \beta_1\cos\theta}\right) + \frac{1 - \cos\left[g_{0,0}(\theta) l\omega/v\right] J_0(2w)}{2(1 - \beta_1\cos\theta)^2} \right\}, \tag{3.8}$$

where $\Delta k_s = k_{s1} - k_{s2}$, the arguments of the Bessel functions are defined in (3.4) and

$$w^2 = \sum_{j=1,2} a_j^2 \sin^2\left(k_{sj} l/2\right) + 2a_1 a_2 \sin\left(k_{s1} l/2\right) \sin\left(k_{s2} l/2\right) \cos\left(\varphi + \Delta k_s l/2\right). \tag{3.9}$$

In the special case $\Delta\varepsilon_2 = 0$ one has $a_2 = 0$ and the only nonzero contribution comes from the terms $m = m_2 = 0$. In this case, (3.8) is reduced to the corresponding spectral angular density for a single acoustic wave, discussed in [8]. Compared to the problem with a single acoustic wave, the presences of the second wave induces new peaks.

By using (3.8), we have made numerical calculations for $I(\omega, \theta)/\hbar$ and for the values of the parameters corresponding to figure 1. The graphs are close to those presented in figure 1. This

2018 JINST 13 C01032

shows that for these values of the parameters and near the peaks the main contribution in (3.8) comes from the part with $m = 0$. In this part, the terms containing $g^2_{m_1,m_2}(\theta)$ in the denominator, responsible for the appearance of the peaks, coincide with those in (3.2). In figure 2, the angular and wavelength dependence of the radiation intensity is displayed in the case of two acoustic waves with the fixed phase shift $\varphi = 0$ (evaluated by formula (3.8)). The values of the parameters are the same as those for figure 1, except the acoustic wave frequency $\nu_{s2} = 40$ MHz. Again, we have the suppression of the peak in the absence of acoustic waves.

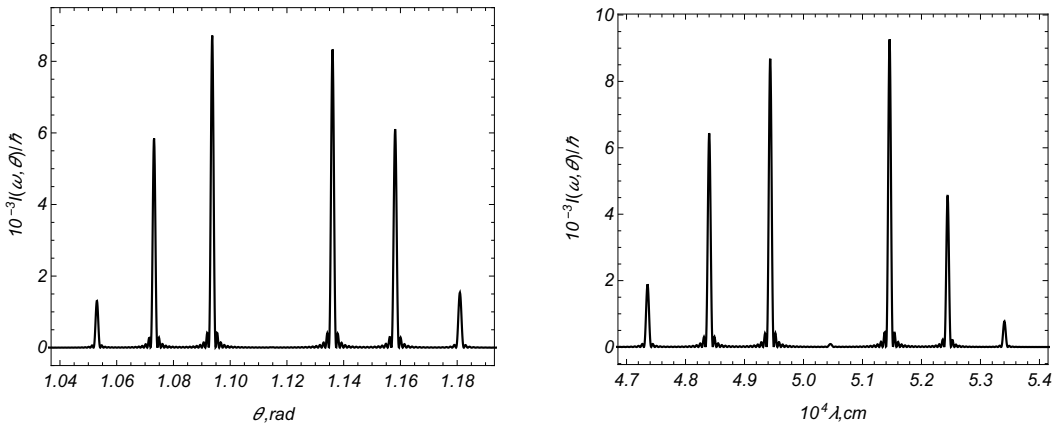

Figure 2. The same as in figure 1 for two acoustic waves with fixed phase shift and for the acoustic wave frequency $\nu_{s2} = 40$ MHz.

4 Conclusion

We have studied the transition radiation on a dielectric plate excited by two acoustic waves. Assuming the validity of the quasi-classical approximation, the vector potential for the radiation field in the forward direction is evaluated. The spectral-angular density of the radiation intensity is investigated for two separate cases. For the first one the phases for separate waves are not correlated and the intensity averaged over these phases is given by (3.2). In the second case the phase shift between the waves is fixed and the expression for the averaged intensity is presented as (3.8). The presence of acoustic waves gives rise to new peaks in both the angular and spectral distributions of the transition radiation intensity. The locations of the peaks, their heights and widths can be controlled by tuning the parameters characterizing the acoustic fields.

References

[1] M.L. Ter-Mikaelian, *High Energy Electromagnetic Processes in Condensed Media*, Wiley Interscience, New York (1972).

[2] G.M. Gharibian and S. Yan, *Rentgenovskoye Perekhodnoye Izluchenie*, Izdatelstvo AN Arm. SSR, Yerevan (1983) [in Russian].

[3] V.L. Ginzburg, V.N. Tsytovich, *Transition Radiation and Transition Scattering*, Adam Hilger, Bristol (1990).

2018 JINST 13 C01032

[4] A.P. Potylitsin, *Electromagnetic Radiation of Electrons in Periodic Structures*, Springer, Berlin (2011).

[5] A.H. Lumpkin, R.J. Dejus and N.S. Sereno, *Coherent Optical Transition Radiation and Self-Amplified Spontaneous Emission Generated by Chicane-Compressed Electron Beams*, *Phys. Rev. ST Accel. Beams* **12** (2009) 040704.

[6] L.G. Sukhikh, G. Kube, S. Bajt, W. Lauth, Yu.A. Popov and A.P. Potylitsyn, *Backward Transition Radiation in the Extreme Ultraviolet Region as a Tool for the Transverse Beam Profile Diagnostic*, *Phys. Rev. ST Accel. Beams* **17** (2014) 112805.

[7] L.S. Grigorian, A.H. Mkrtchian and A.A. Saharian, *Transition radiation in an ultrasonic superlattice*, *Nucl. Instrum. Meth.* **B 145** (1998) 197.

[8] A.R. Mkrtchyan, V.V. Parazian and A.A. Saharian, *Optical transition radiation in presence of acoustic waves*, *Mod. Phys. Lett.* **B 24** (2010) 2693 [arXiv:0912.4111].

[9] A.R. Mkrtchyan, V.V. Parazian and A.A. Saharian, *Optical transition radiation in presence of acoustic waves for an oblique incidence*, *Int. J. Mod. Phys.* **B 26** (2012) 1250036 [arXiv:1109.4188]

[10] A.R. Mkrtchyan, A.P. Potylitsyn, V.R. Kocharyan and A.A. Saharian, *Transition Radiation on a Dynamic Periodic Interface*, *Phys. Rev.* **E 93** (2016) 022117.

2018 JINST 13 C01032